Droop Control Operation Strategy for Advanced DC Converter-Based Electrical Railway Power Supply Systems for High-Speed Lines

D. Serrano-Jiménez*, S. Castano-Solís**. E. Unamuno***, J.A. Barrena***
*ETSIME-Universidad Politécnica de Madrid, Ríos Rosas 21, 28003 Madrid, Spain.
**ETSIDI–Universidad Politécnica de Madrid, Ronda de Valencia 3, 28013 Madrid, Spain.
***EPS-Mondragón Unibertsitatea, Loramendi 4, 20500 Mondragón, Spain

***Abstract*—Advanced DC converter-based electrical railway power supply systems are very promising power supply configurations for the electrification of high-speed lines. Their full controllable converter-based traction substations along with its continuous catenary, enable the reduction of power quality issues while providing an active power management. However, the power operation performance of these new configurations relies on the development of appropriate control systems. In this sense, this paper introduces a novel operation strategy based on a droop control scheme capable of adapting the power sharing between traction substations without any traffic information. The power operation performance of a simple and complex advanced DC converter-based system following the strategy proposed has been analyzed and compared with the conventional electrification approach. According to the results obtained, the operation strategy presented can adequately control the power flow in the railway grid for both scenarios.**

***Index Terms*— Advanced DC converter-based systems, distributed voltage, droop control, electrical railway power supply systems (ERPSS), hierarchical control, master-slave, power flow.**

I. Introduction

Conventional transformer-based systems are robust and reliable electrical power supply systems for the electrification of high-speed lines. They typically consist of a catenary line divided into isolated electrical sections fed from the utility grid by means of single-phase transformer traction substations. This electrification scheme presents important quality issues such as power imbalance or harmonics injection [1] and avoids the possibility of an active the power flow control in the railway grid. In the light of these difficulties, researchers have been proposing different technological solutions capable of overcoming the aforementioned limitations [2]. One of the most promising ones is the so-called advanced DC converter-based system [3].

Advanced DC converter-based systems consist of a series of voltage source converter (VSC) stations [4] that feed a continuous catenary. The use of modern electronic switches combined with the use of a continuous catenary configuration enables the active control of the power flow in the railway grid. As in the conventional transformer-based system, advanced DC converter-based systems can have a monovoltage or a bivoltage catenary arrangement. For the latter case, the use of DC/DC autoconverter stations that distribute the current between the positive and negative conductors is necessary [5].

The operation of advanced DC converter-based systems is essentially determined by the control system implemented. In general, there are two opposite control schemes in literature: centralized and decentralized [6]. The centralized approach is based on the use of a single central controller that defines the action references for the different distributed resources according to the operation objective defined. On the contrary, decentralized approaches perform the operation of the system by means of local controllers placed at each distributed resource. In contrast to the centralized approach, in decentralized systems, the local controller typically only has the information of its corresponding distributed resource.

The implementation of a fully centralized scheme or a fully decentralized scheme is often avoided [7]. On the first hand, fully centralized control requires the use of fast communication channels and powerful computational resources that makes its implementation very costly for extended geographical areas such as railway systems. Furthermore, the operation of the whole system relies on the performance of a single controller. On the other hand, fully decentralized control provides lower cost and higher reliability, but it complicates enormously the achievement of global objectives since the available information is limited to the local environment. Taking all these considerations into account, researchers have opted for the development of hierarchical control systems that combines both approaches [8].

Hierarchical control divides the operation of the grid into different levels which have decoupled time scales. In this sense, higher management levels have longer time scales and provide supervisory control over lower control levels. This disaggregation is very advantageous since the different control actions require very different time responses. The number and actions of these levels differs in the literature, but in general, they all include two broad levels where the lower level is in charge of maintaining the power balance in the grid and the higher level defines the power sharing of the grid. Figure 1 shows the application of this scheme to an advanced DC converter-based ERPSS with a bivoltage catenary configuration.

The development of operation strategies for electrical systems with power converters, such as high voltage direct current grids [9], [10] or microgrids [11], [12], has been extensively discussed in the literature, but their application to advanced converter-based ERPSS has been little explored. The few studies existing [13], [14] are mainly focused on the performance and stability of the local controllers, and thus, they do not provide any insight about possible power flow distribution strategies between the traction substations and the trains. In this situation, this paper presents a new strategy for the central controller based on a droop control scheme capable of improving the performance and reliability of the railway power flow operation with respect to the conventional transformer-based electrification approach. This study was initiated in [15], and now it is extended and completed for a bivoltage advanced DC converter-based system. To the best of the author's knowledge, it is the first time that the power operation of this type of system is thoroughly described.

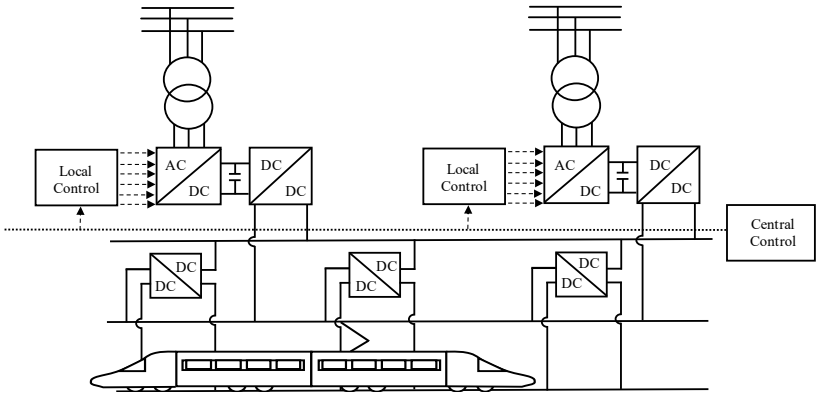

Figure 1. Hierarchical control system for advanced DC converter-based systems.

This paper has been organized into five sections. The first section is an introduction to advanced DC converter-based systems and their operation control schemes. In the second section, the control strategy proposed is comprehensively formulated and discussed. The third section describes the electrical simulation model used in the paper. In the fourth section, the operation of advanced DC converter-based systems using the control strategy proposed is thoroughly analyzed for a simple and for a complex simulation scenario and compared with the conventional electrification approach. Finally, the fifth section addresses the main conclusions of the paper.

II. Operation Strategy

The development of advanced converter-based power supply systems for high-speed lines brings new possibilities for the electrical operation of railway grids [16]. In this sense, this paper presents a novel strategy capable of increasing or decreasing the power sharing between the traction substations depending on the utility grid requirements regardless of the traffic condition existing. It is noted that when the utility grid does not require any support from the railway grid, the power demanded by the trains should be distributed according to the distance between the trains and the traction substations in order to reduce the power losses in the catenary.

To develop this operation strategy, the central controller must provide the right references to the local controllers. Depending on the local control approach, the central controller must provide different information. According to [17], there are two main local control modes: grid forming and grid following. In the grid forming mode, the converters behave as an ideal voltage source that sets the value of the voltage regardless of the power delivered. Alternatively, in the grid following mode, the converters behave as an ideal current source that sets the value of the current according to the power demand and the voltage level existing. Finally, both modes can support the grid regulating the voltage or the current according to the grid condition. Depending on the combination of the local control modes previously described, three principal control schemes can be defined: master-slave, direct voltage control, and droop control.

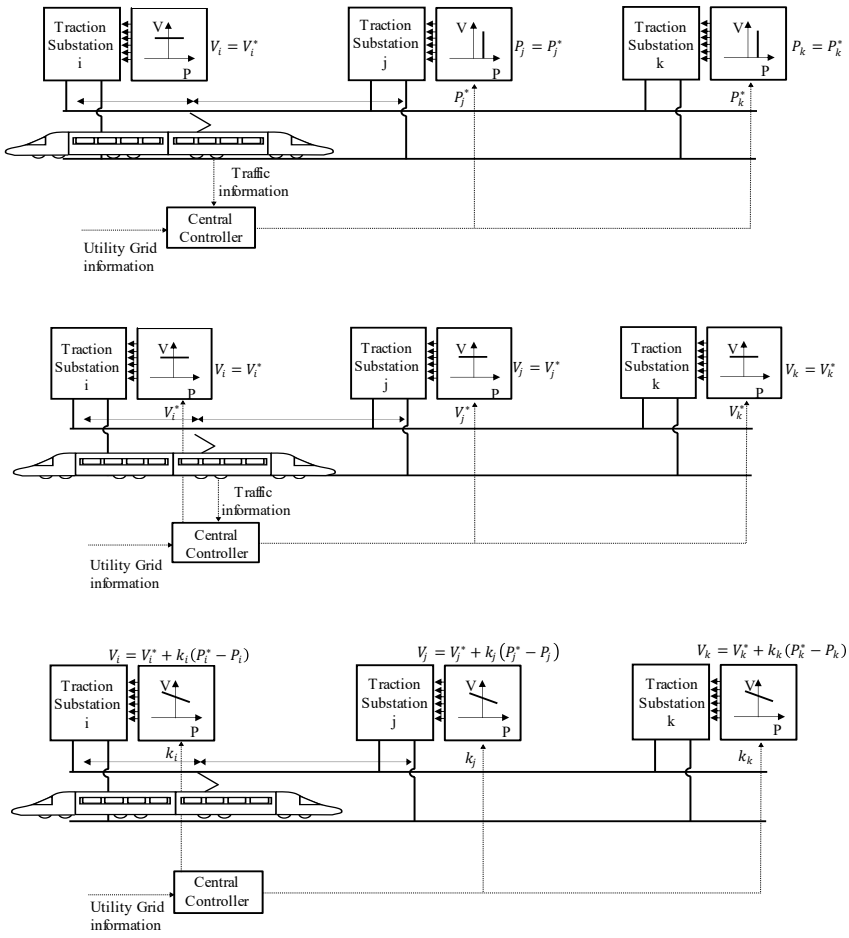

Figure 2. Control schemes for electrical power sharing. a) Master-Slave b) Direct Voltage Control c) Droop Control.

In the master-slave approach, Figure 2.a, one converter, called master, is controlled in grid forming mode, while the rest of the converters, called slaves, are controlled in grid following mode. The application of this scheme to advanced railway grids is not very convenient. On the first hand, the power balance is performed by a single converter, reducing the reliability and requiring the connection of the master unit to a strong grid. On the other hand, the power sharing depends on the central controller performance that must update the power references of the slave converters for different traffic conditions. Accordingly, this scheme needs a fast communication channel that increases the cost significantly.

In the direct voltage control scheme [18], Figure 2.b, all converters have implemented a grid forming mode. By simply setting the same voltage in all the traction substations, the power demanded by the trains will be distributed among the power converters according to the corresponding distance between the trains and the substations. Although it seems a very simple and efficient solution, it presents important drawbacks. The first and most reported one is the possibility of existing circulating currents. Since the voltage is imposed externally, small errors in the magnitude definition can lead to undesirable power flow distributions. Another important disadvantage is the complexity to define power flow distributions different from this one. In this case, the new voltage sets should be calculated by means of an optimal power flow that must be run every time the traffic condition varies.

In the droop control approach, Figure 2.c, all converters have implemented a grid forming mode with grid supporting functionality. As it is generally known, the voltage set by the converter changes with the power delivered according to the droop parameter defined, *k*. This control law is very useful for the development of the operation strategy described since it can regulate the power sharing considering the distance between the trains and the traction substations without any traffic information. In order to illustrate it, a simple example of two substations and a single train is used, Figure 3. The resistances seen from each traction substation are $a \cdot R_T$ *and* $(1\text{-}a) \cdot R_T$; where R_T represents the total impedance of the section and *a,* the relative position of the train. The voltage drop in the train has been divided into two parts. The first part is a virtual voltage drop due to the droop control, represented as a virtual resistance R_v, and the second part corresponds to the voltage drop due to the line impedance, R_T.

When the droop coefficients tend to zero, the voltage drop in the virtual impedance can be neglected, and the electrical power provided by each traction substation is defined by the line impedance existing between the train and the substations. Accordingly, the power sharing will be determined by the ratio $(1\text{-}a)/a$. On the other hand, as the droop coefficients increase, the effect of the line impedance is reduced, and the power provided by each traction substation tends to be equal. Ideally, if the resistance of the line is negligible, the power sharing is given by the ratio k_{v2}/k_{v1}. Figure 3 shows the power sharing analysis previously described. It is noted that in order to maintain the train position information in the power sharing, the droop coefficients of the traction substations must have the same value.

These results are very interesting since they show how the power sharing between the traction substations can be controlled by simply modifying the values of the droop parameters. For normal situations where the utility grid does not require any support from the railway grid, the droop parameter will be fixed as low as possible in order to increase the system efficiency. On the other hand, under any possible utility grid support requirement, the droop parameters can be increased in order to raise the power cooperation between traction substations. Finally, it is important to highlight that the power delivered by any traction substation can be fixed to a maximum value if needed.

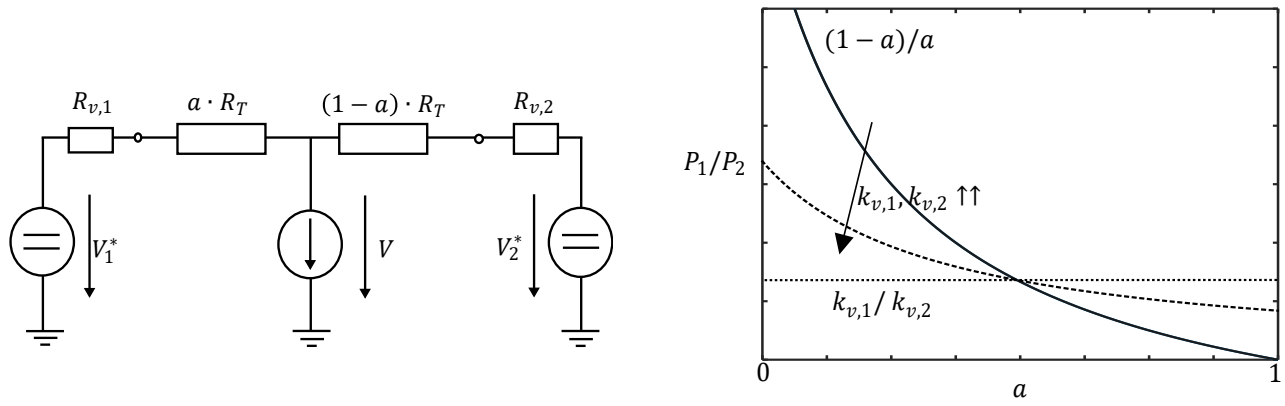

Figure 3. Power sharing analysis for droop control operation strategy.

III. SIMULATION MODEL

The performance of the control strategy is calculated by means of a power flow analysis. It is noted that the power flow distribution may also be calculated by a time-domain simulation, but it complicates the problem unnecessary since we only need the steady state values to evaluate the strategy performance. The power flow analysis with converter control is not a trivial task [19]. The conventional nodal formulation used in operation studies presents several limitations to incorporate element models that include controllable voltage sources and non-grounded connections. To overcome these shortcomings, a modified nodal analysis is used [20].

This technique uses not only the node voltages as variables but also some currents. This fact eliminates the aforementioned limitations and makes it very simple the implementation of more converter controls such as the droop. On the downside, this approach increases the number of unknowns to calculate. The following subsections describe the element models used and the system formulation. It is important to highlight that this simulation model has previously been validated for the Spanish high-speed railway line Madrid-Valencia.

- *Catenary model.*

The catenary is one of the most important parts of the model. It is represented by means of a multidimensional equivalent lumped π network whose electrical parameters can be calculated using the Carson equations and the Maxwell potential coefficients [21]. The representation of all catenary conductors is seldom needed, and they are normally grouped and reduced to equivalent ones according to their voltage level using the Kron reduction. Considering this information, the catenary formulation for a bivoltage configuration is finally reduced to a 2x2 admittance matrix. Figure 4.a shows the equivalent circuit for a catenary section defined by the nodes i and j for the equivalent positive conductor, and the nodes m and n for the equivalent negative conductor. The variables Z_{pp} and Z_{nn} stand for the positive and negative equivalent conductor self-impedance and, Z_{pn} and Z_{np} for the mutual ones. It is noted that in the advanced DC converter-based system, the inductive and capacitive effects of the lines are not considered.

- *Traction substation transformer and autotransformer models.*

The most common traction substation transformer for bivoltage catenary configurations is a single-phase two-winding transformer with the secondary central point grounded. This element is usually modeled as single-phase three-winding transformer whose admittance matrix can be calculated by means of three short-circuit tests. Figure 4.b shows the equivalent circuit for the traction transformer used, where the nodes i and j define the primary winding, nodes m and n, the secondary winding, and nodes

o and *p*, the tertiary winding. The variables Z_{pp}, Z_{ss} and Z_{tt} stand for the primary, secondary and tertiary winding self-impedance and, Z_{ps}, Z_{pt} and Z_{st} for the mutual ones.

The autotransformers are single-phase transformers whose primary and secondary windings are connected in series. The admittance matrix of this element can be easily obtained by means of a single short-circuit test. Figure 4.c shows the equivalent circuit for the autotransformer used, where the nodes *i* and *j* defines the primary winding, and nodes *m* and *n,* the secondary. The variables Z_{pp} and Z_{ss} stand for the primary and secondary winding self-impedance and, Z_{ps} and Z_{ps} for the mutual ones.

- *Traction substation converter and autoconverter models.*

Converter traction substations are the main elements in the new advanced DC converter-based ERPSSs. Each station is composed of a three-phase VSC. Since the study is focused on the railway operation, only the railway side of the converter is considered. According to the control strategy described in Section II, the converter substation will be modeled as a controllable voltage source whose power is proportional to the voltage droop according to the droop parameter selected, k_x. This behavior is mathematically represented in (1), where the first part corresponds to the power of the converter in terms of the current I_x and node terminal voltages V_i and V_j, and the second part to the power according to the droop characteristic adapted to the element notation shown in Figure 4.d.

$$\left(V_i - V_j\right) \cdot I_x + (1/k_x) \cdot \left(V_x^* - V_i + V_j\right) = 0 \tag{1}$$

The autoconverters are in charge of performing the autotransformer functionalities in AC bivoltage catenary schemes. Accordingly, the autoconverter is modeled as two controlled dependent DC sources, where their voltage must be equal with opposite sign, and the power demanded by one source must be equal to the power injected by the other plus the power converter losses. Although there are simpler autoconverter representations, this formulation enables to consider or not the power converter losses easily if needed. (2) and (3) define the performance of the model presented in figure 4.e. As noticed, they model the behavior of an ideal transformer, and the converter power losses are not included.

$$\left(V_i - V_j\right) \cdot I_x + (V_m - V_n) \cdot I_y = 0 \tag{2}$$

$$\left(V_i - V_j\right) + (V_m - V_n) = 0 \tag{3}$$

- *Train model*

The representation of the train for operation studies has been extensively discussed in literature. In the earliest times, trains were represented as a constant impedance or as a current source. These models are especially convenient for short circuit studies, but they are not very realistic in power flow approaches. The VSC converters used in modern trains enable to control the electrical power as desired. Thus, the most common and realistic representation is as a power source. Therefore, the train is represented as a power source whose behavior is defined in (4) and (5), where V_i and V_j are the terminal node voltages, I_x, the current injected by

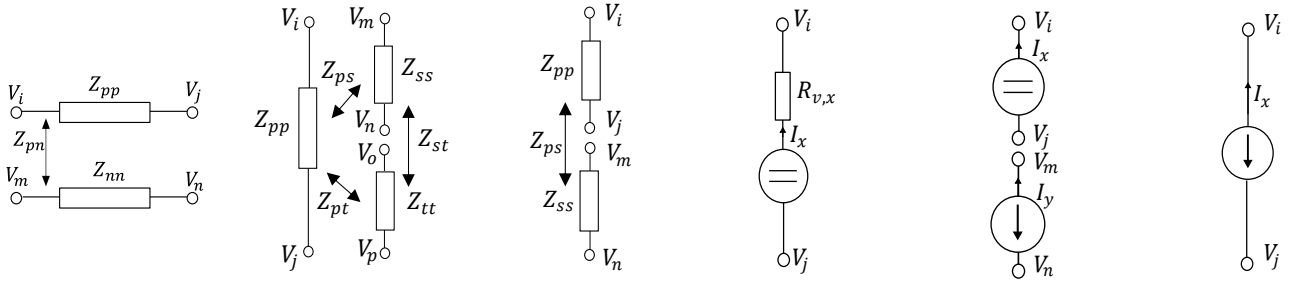

a) Catenary | *b) Transformer traction substation* | *c) Autotransfomer* | *d) Converter traction substation* | *e) Autoconverter* | *f) Train*

Figure 4. Element equivalent circuits.

the train and, P_x and Q_x, the active and reactive power demanded by the train. For the advanced DC converter-based, only the first equation is needed.

$$\Re\{(V_i - V_j) \cdot I_x^*\} - P_x = 0 \tag{4}$$

$$\mathbb{I}\{(V_i - V_j) \cdot I_x^*\} - Q_x = 0 \tag{5}$$

- *System formulation*

Once the element models are defined, the railway system can be created by means of their interconnection according to the electrification scheme. Considering all this information, the electrical system equations can be defined by means of the current balance for each node of the system and the control equations of the active sources. Finally, all equations are solved by means of a Newton-Raphson numerical algorithm.

IV. Simulation results

This section analyzes and compares the electrical operation performance of advanced DC converter-based systems following the control strategy presented with the conventional transformer-based approach. For the sake of providing a comprehensive understanding, the system operation is firstly studied for a simple test case and subsequently extended to a more realistic and challenging simulation scenario.

A. Simple test case

The simple test case consists of the electrification of a 60 km railway line with a bivoltage catenary configuration. The catenary is fed from two traction substations placed at the beginning and the end of the line. There is an autotransformer or an autoconverter every 10 km of the catenary depending on the electrification approach studied. It is noted that for transformer-based case, the catenary is divided into two isolated electrical sections since the traction substations are normally connected to different phases to

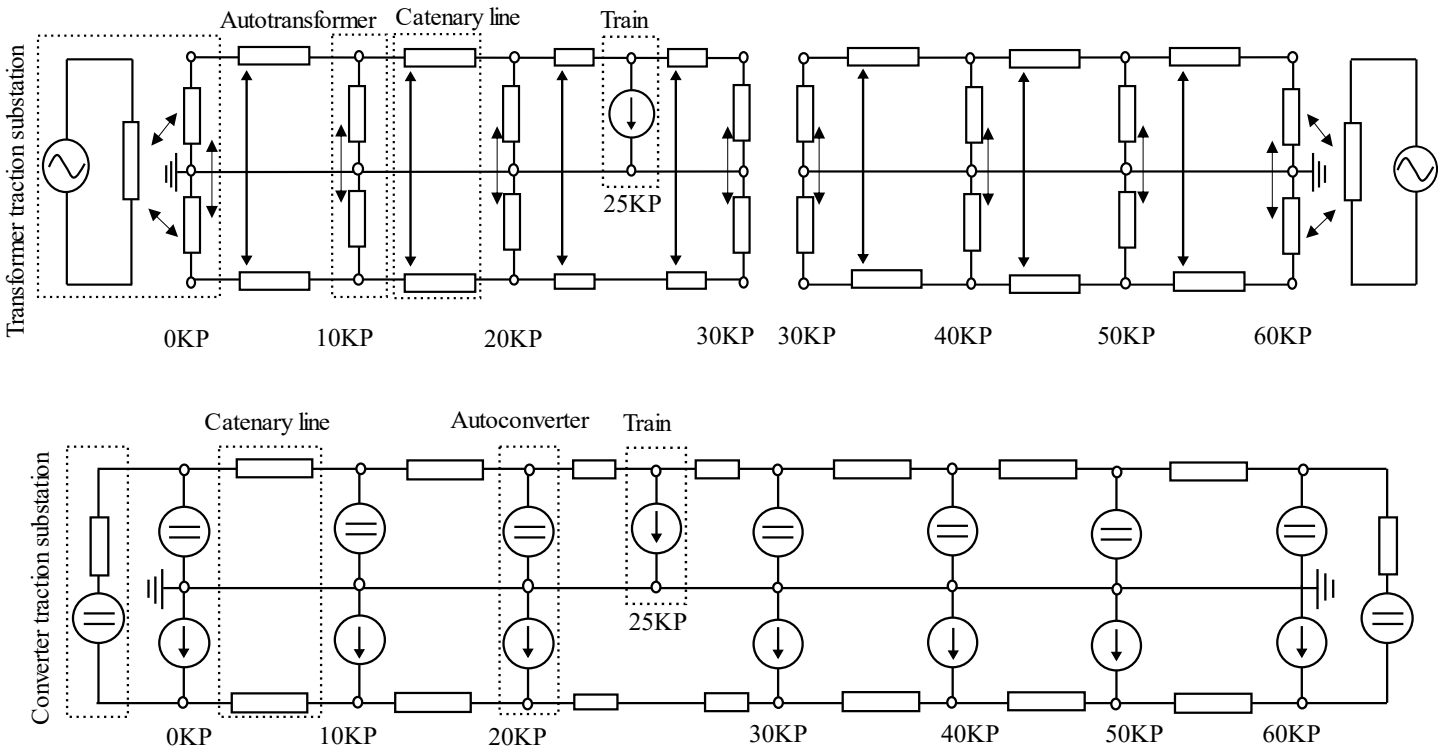

Figure 5. Equivalent circuit. Simple test case. a) Transformer-based system. b) Converter-based system.

reduce the power imbalance. The equivalent circuits of the test case for both electrification approaches when the train is placed at 25KP are shown in Figure 5.

To compare the performance of both electrification approaches, the droop parameters of the advanced DC converters-based traction substation have been set to zero since the transformer-based objective is reducing the catenary voltage drop. The traffic is defined as a single train that demands a constant power of 10 MW for any position. The catenary is assumed to be working at 25 kV and the utility grid has been considered ideal. The data of the transformers and catenary line are listed in Table 1.

Autotransformer admittance (1/Ω)	*Autotransformer admittance* (1/Ω)	Catenary Line Impedance (Ω/m)
$\begin{bmatrix} -0.32j & 0.32j \\ 0.32j & -0.32j \end{bmatrix}$	$\begin{bmatrix} -0.014j & 0.062j & 0.062j \\ 0.062j & -2.194j & 1.646j \\ 0.262j & 1.464j & -2.194j \end{bmatrix}$	$\begin{bmatrix} 0.11+0.28j & 0.07+0.12j \\ 0.07+0.12j & 0.13+0.31j \end{bmatrix} \cdot 10e-4$

Table 1. Element impedance values.

- *Voltage and current analysis.*

Figure 6 illustrates the voltage and the current geometrical locus between the maximum and the minimum values obtained for the equivalent positive and negative conductors over their length for all the train positions. The four upper charts correspond to the transformer-based configuration while the four bottom ones to the converter-based configuration. The dashed lines in the charts are the voltage and current distributions when the train is placed at the 25KP.

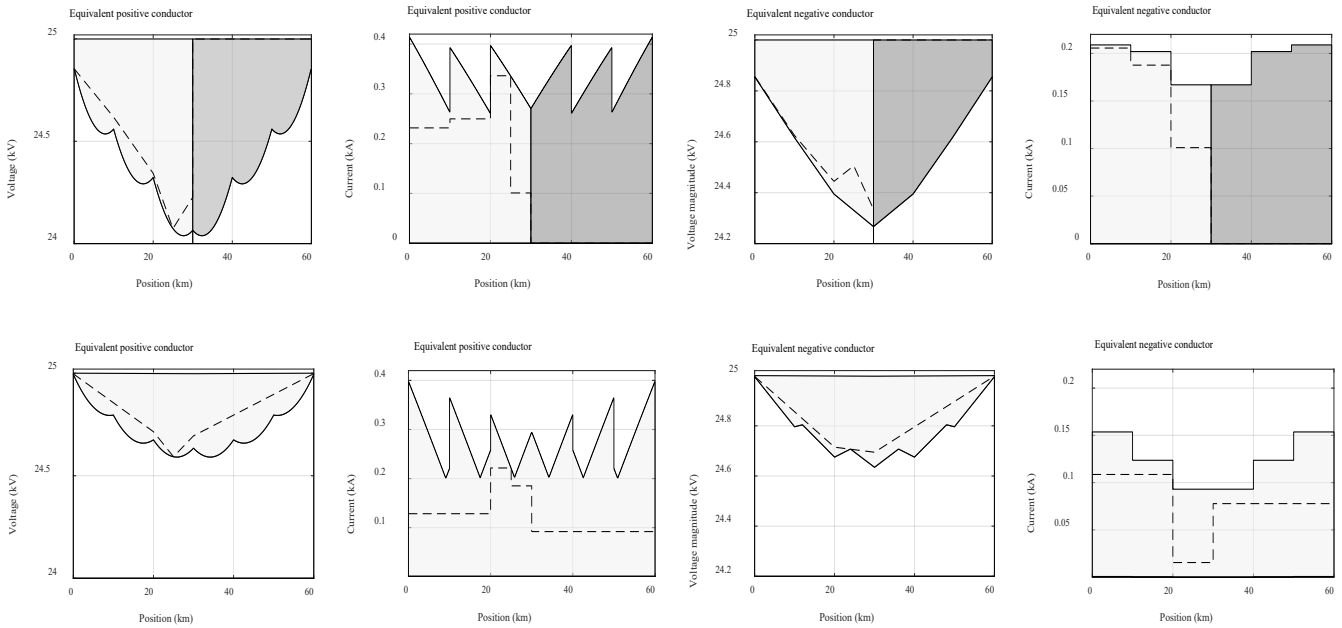

Figure 6. Voltage and current analysis. Simple test case.a) Transformer-based systen (upper) b) Converter-based system (bottom).

As it is shown, the voltage in the catenary decreases from the traction substations to the train. It is noted that for the transformer-based system, only one traction substation can feed the train. The voltage variation rate changes at the autotransformer or autoconverter positions since they perform a new current distribution in the conductors. For the converter-based system, only the autoconverters adjacent to the train work at each moment since they have been considered ideal and perform a perfect current balance. Finally, the coupling between the catenary conductors for the transformer-based system can be seen in the voltage increase experienced in the negative conductor between the two autotransformers adjacent to the train.

Comparing the transformer-based performance with the converter-based one, the voltage drop in the catenary has been significantly reduced due to the possibility of feeding the trains from both traction substations. This fact makes it possible to increase the distance between traction substations and thus, reducing their number and the cost of the system. It can be argued that this could also be achieved by means of a transformer-based system as long as the traction substation transformers were connected to the same phases. However, this solution would require the connection of the substation to stronger utility grids.

- *Power sharing analysis*

This section analyses the operation strategy for advanced DC converter-based systems proposed in the paper. Only the case for the advanced DC is considered here, since in transformer-based configurations, there is not possible any power sharing between traction substations. Figure 7.a shows the active power delivered by the traction substations for all the train positions for a droop parameter value of 1/e-4 (V/W). It can be observed that the power supplied decreases as the train runs away from the traction substation and both traction substations are providing power simultaneously.

As it was described before, if the utility grid requires to reduce the power demanded at the most loaded connection points, the railway operator can rise the droop parameter, increasing the power cooperation between traction substations. In order to analyze this situation, the test case has been simulated for four different droop parameter values: 1/1e-4V/W, 1/2e-4V/W, 1/3e-4V/W and 1/4e-4 V/W. Figure 7.b proves that when the droop coefficients are increased, the power sharing between traction substations grows. According to these results, the proposed strategy can control the power sharing between the traction substations without information about the traffic conditions by simply increasing or decreasing the droop parameters of the traction substations.

Finally, Figure 7.c and Figure 7.d describes the power distribution and the power sharing performance respectively when there is a power limitation on one traction substation. As it can be observed, the power supplied from traction substation two increases as the train runs away from traction substation one until it reaches the maximum power limit of 4MW. In this moment, the traction substation one is in charge of providing the rest of the power required. This example shows the versatility of advanced DC converter-based systems.

B. Complex test case

This section analyzes and compares the electrical operation performance of advanced DC converter-based systems following the control strategy presented with the conventional transformer-based approach for a more complex and challenging scenario. To this end, the Madrid-Valencia high-speed railway line configuration is used as reference. This line is currently electrified using a conventional transformer-based scheme composed of thirteen independent electrical sections and seven traction substations.

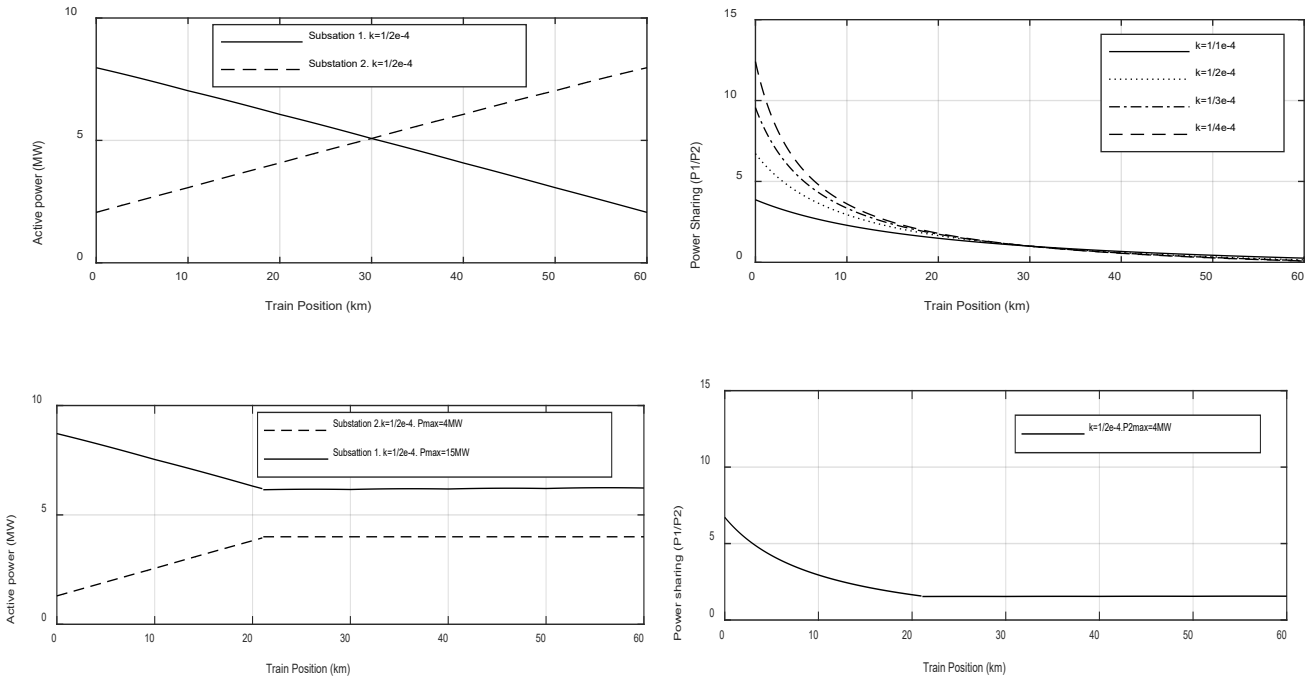

Figure 7. Power distribution and power sharing analysis. Simple test case.

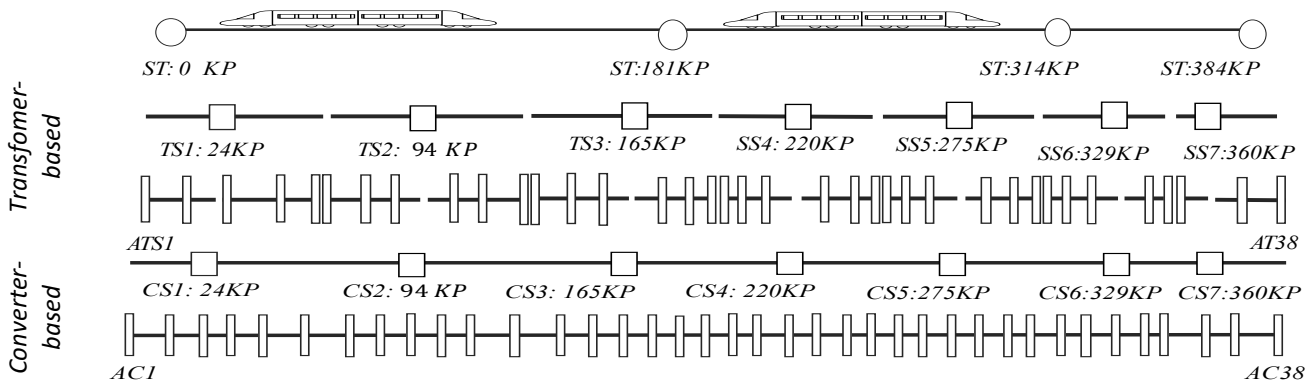

Figure 8. Test case electrical power supply schemes.

The advanced DC converter-based electrification scheme has been performed by simply replacing the current transformer-based traction substations with the corresponding converter-based ones and connecting all the electrical sections. Furthermore, the autotransformers have been substituted with equivalent DC/DC converters. According to all this information, the electrification schemes for both configurations are shown in Figure 8. The data of the transformers and catenary line are listed in Table 2. Finally, it is important to highlight that the number of converter traction substations needed, and their situation might be lower than in the conventional scheme, but this problem is not considered in this paper. A simple but rigorous analysis of this issue can be found in [22], where the distance between traction substation is determined according to the voltage level.

To perform the analysis, the system has been simulated for a single instant, where there are four trains placed at positions: 62,45KP, 91.66KP, 202,41KP and 315.65KP that are consuming an active power of 11,15MW, 8.96MW, 7.25 MW and 11,15MW, respectively. The droop parameters of all traction substations have been initially set to 1e-5V/W.

Autotransformer admittance (1/Ω)	*Autotransformer admittance* (1/Ω)	Catenary Line Impedance (Ω/m)
$\begin{bmatrix} 0.062-0.307j & -0.062+0.307j \\ -0.062+0.307j & 0.062-0.307j \end{bmatrix}$	$\begin{bmatrix} -0.052j & 0.122j & 0.122j \\ 0.122j & -2.194j & 1.646j \\ 0.122j & 1.464j & -2.194j \end{bmatrix}$	$\begin{bmatrix} 0.06+0.18j & 0.02+0.09j \\ 0.02+0.09j & 0.13+0.29j \end{bmatrix} \cdot 10e-4$

Table 2. Element impedance values.

Figure 9 shows the voltage (equivalent positive conductor) and the power distribution obtained for the transformer-based (upper) and the converter-based (bottom) configurations. As expected, the transformer-based system presents higher voltage drops than the converter-based system and only one traction substation is feeding the same train at the same time due to the catenary sectioning. This fact makes necessary the use of traction substations with higher power ratings, increasing the cost of the system.

In order to validate the operation strategy, the power provided by each traction substation has been studied for three different droop parameter values: 1000/60 V/MW, 2000/60 V/MW and 3000/60 V/MW. As it can be observed in Figure 10, the power sharing increases as the droop parameter does, so that the power differences between the most loaded and less loaded substations are reduced. This issue validates the control strategy proposed for larger and more complex systems. However, these droop values do not allow to obtain a significant power cooperation. It has been simulated for lower voltage droop parameters, but the algorithm fails to converge. The reason behind this issue is that the solution is approaching to a maximum as the voltage droop parameters are increased, and the Jacobian matrix turns into a singular matrix.

Finally, in order to analyze the reliability of the new operation points reached by the new droop parameters, the voltage distribution of the equivalent positive conductor is shown in Figure 10.b As it was noticed before, a higher droop parameter leads to higher voltage drops in the conductor. However, despite the higher voltage drop observed, the values are always within the admissible levels defined by the standard [23].

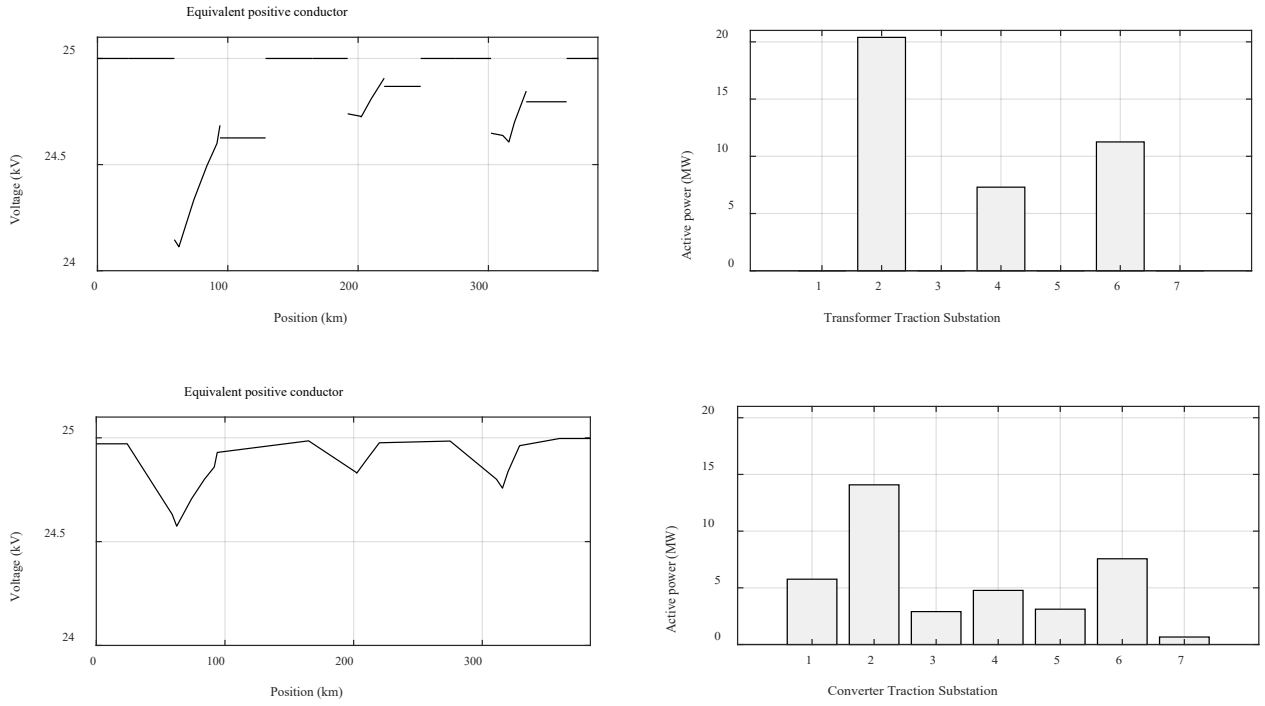

Figure 9. Voltage and power analysis. Complex test case.a) Transformer-based system (upper) b) Converter-based system (bottom).

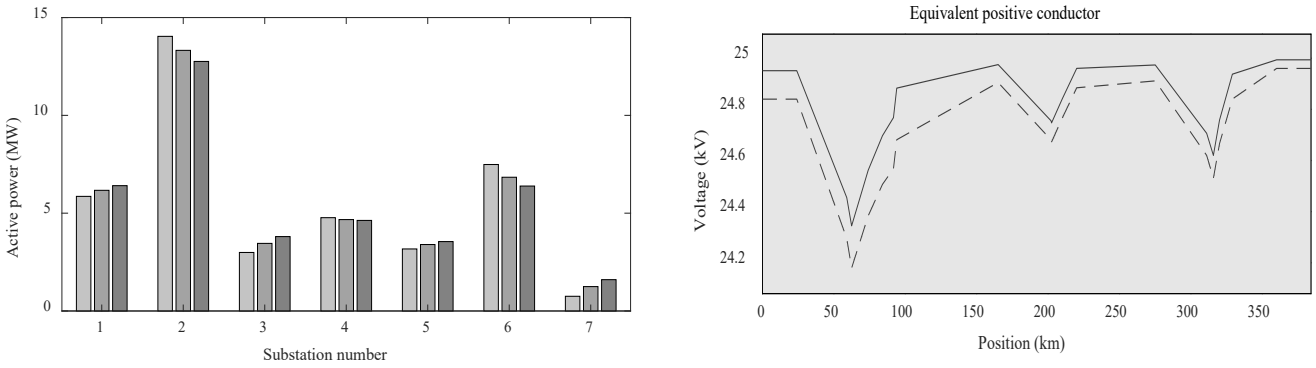

Figure 10. Power sharing analysis. Complex test case.

V. CONCLUSIONS

Advanced DC converter-based systems are a good option for the electrification of high-speed railway lines. Their full controllable converter stations along with its continuous catenary enable to control actively the electrical power in the railway grid. Thus, the implementation of efficient and reliable operation control strategies becomes vital.

According to the analysis performed, the hierarchical control system is the most suitable option for advanced converter-based railway system since they combine the advantages of centralized and decentralized control approaches. Among the different local control techniques, droop control-based methods are especially convenient for railways. As it was described, the modification of the droop parameter enables to define the cooperation between the traction substations without the need to consider the traffic conditions.

According to the results obtained, the element models used in the paper to study the railway operation describe coherent voltage and current behaviors. Furthermore, the theoretical conclusions of the control strategy are confirmed by the simulation results. This control strategy is valid for simple and complex electrification schemes.

VI. REFERENCES

[1] A. T. Langerudy, A. Mariscotti, and M. A. Abolhassani, "Power Quality Conditioning in Railway Electrification: A Comparative Study," *IEEE Trans. Veh. Technol.*, vol. 66, no. 8, pp. 6653–6662, Aug. 2017, doi: 10.1109/TVT.2017.2661820.

[2] D. Serrano-Jiménez, L. Abrahamsson, S. Castaño-Solís, and J. Sanz-Feito, "Electrical railway power supply systems: Current situation and future trends," *Int. J. Electr. Power Energy Syst.*, vol. 92, 2017, doi: 10.1016/j.ijepes.2017.05.008.

[3] A. Gomez-Exposito, J. M. Mauricio, and J. M. Maza-Ortega, "VSC-Based MVDC Railway Electrification System," *IEEE Trans. Power Deliv.*, vol. 29, no. 1, pp. 422–431, Feb. 2014, doi: 10.1109/TPWRD.2013.2268692.

[4] P. Simiyu and I. E. Davidson, "MVDC Railway Traction Power Systems; State-of-the Art, Opportunities, and Challenges," *Energies 2021, Vol. 14, Page 4156*, vol. 14, no. 14, p. 4156, Jul. 2021, doi: 10.3390/EN14144156.

[5] F. Wang, Z. Lei, X. Xu, and X. Shu, "Topology deduction and analysis of voltage balancers for DC microgrid," *IEEE J. Emerg. Sel. Top. Power Electron.*, vol. 5, no. 2, pp. 672–680, Jun. 2017, doi: 10.1109/JESTPE.2016.2638959.

[6] D. E. Olivares *et al.*, "Trends in Microgrid Control," *IEEE Trans. Smart Grid*, vol. 5, no. 4, pp. 1905–1919, Jul. 2014, doi: 10.1109/TSG.2013.2295514.

[7] X. Lu *et al.*, “Hierarchical distributed control approach for multiple on-site DERs coordinated operation in microgrid,” *Int. J. Electr. Power Energy Syst.*, vol. 129, p. 106864, Jul. 2021, doi: 10.1016/J.IJEPES.2021.106864.

[8] J. M. Guerrero, J. C. Vasquez, J. Matas, L. G. de Vicuna, and M. Castilla, “Hierarchical Control of Droop-Controlled AC and DC Microgrids—A General Approach Toward Standardization,” *IEEE Trans. Ind. Electron.*, vol. 58, no. 1, pp. 158–172, Jan. 2011, doi: 10.1109/TIE.2010.2066534.

[9] A. M. Bouzid, J. M. Guerrero, A. Cheriti, M. Bouhamida, P. Sicard, and M. Benghanem, “A survey on control of electric power distributed generation systems for microgrid applications,” *Renewable and Sustainable Energy Reviews*, vol. 44. Elsevier Ltd, pp. 751–766, Apr. 01, 2015, doi: 10.1016/j.rser.2015.01.016.

[10] T. Dragicevic, X. Lu, J. C. Vasquez, and J. M. Guerrero, “DC Microgrids - Part I: A Review of Control Strategies and Stabilization Techniques,” *IEEE Transactions on Power Electronics*, vol. 31, no. 7. Institute of Electrical and Electronics Engineers Inc., pp. 4876–4891, Jul. 01, 2016, doi: 10.1109/TPEL.2015.2478859.

[11] J. Beerten, O. Gomis-Bellmunt, X. Guillaud, J. Rimez, A. Van Der Meer, and D. Van Hertem, “Modeling and control of HVDC grids: A key challenge for the future power system,” Feb. 2014, doi: 10.1109/PSCC.2014.7038505.

[12] F. D. Bianchi, J. L. Domínguez-García, and O. Gomis-Bellmunt, “Control of multi-terminal HVDC networks towards wind power integration: A review,” *Renewable and Sustainable Energy Reviews*, vol. 55. Elsevier Ltd, pp. 1055–1068, Mar. 01, 2016, doi: 10.1016/j.rser.2015.11.024.

[13] X. Yang, H. Hu, Y. Ge, S. Aatif, Z. He, and S. Gao, “An Improved Droop Control Strategy for VSC-Based MVDC Traction Power Supply System,” *IEEE Trans. Ind. Appl.*, vol. 54, no. 5, pp. 5173–5186, Sep. 2018, doi: 10.1109/TIA.2018.2821105.

[14] X. Zhu, H. Hu, H. Tao, Z. He, and R. Kennel, “Stability Prediction and Damping Enhancement for MVDC Railway Electrification System,” *IEEE Trans. Ind. Appl.*, pp. 1–1, May 2019, doi: 10.1109/tia.2019.2916376.

[15] D. Serrano-Jimenez, J. Sanz-Feito, and S. Castano-Solis, “Modeling, Simulation and Analysis of an Advanced Mono-Voltage DC Converter-Based Electrical Railway Power Supply System for High Speed Lines,” in *2017 IEEE Vehicle Power and Propulsion Conference, VPPC 2017 - Proceedings*, 2018, vol. 2018-Janua, doi: 10.1109/VPPC.2017.8331002.

[16] E. Pilo De La Fuente, S. K. Mazumder, and I. G. Franco, “Railway Electrical Smart Grids: An introduction to next-generation railway power systems and their operation,” *IEEE Electrif. Mag.*, vol. 2, no. 3, pp. 49–55, 2014, doi: 10.1109/MELE.2014.2338411.

[17] E. Unamuno and J. A. Barrena, “Hybrid ac/dc microgrids - Part II: Review and classification of control strategies,” *Renewable and Sustainable Energy Reviews*, vol. 52. Elsevier Ltd, pp. 1123–1134, Aug. 22, 2015, doi: 10.1016/j.rser.2015.07.186.

[18] R. Teixeira Pinto, P. Bauer, S. F. Rodrigues, E. J. Wiggelinkhuizen, J. Pierik, and B. Ferreira, “A Novel Distributed Direct-Voltage Control Strategy for Grid Integration of Offshore Wind Energy Systems Through MTDC Network,” *IEEE Trans. Ind. Electron.*, vol. 60, no. 6, pp. 2429–2441, Jun. 2013, doi: 10.1109/TIE.2012.2216239.

[19] G. Agundis-Tinajero, J. Segundo-Ramírez, N. Visairo-Cruz, M. Savaghebi, J. M. Guerrero, and E. Barocio, “Power flow modeling of islanded AC microgrids with hierarchical control,” *Int. J. Electr. Power Energy Syst.*, vol. 105, pp. 28–36, Feb. 2019, doi: 10.1016/J.IJEPES.2018.08.002.

[20] Chung-Wen Ho, A. Ruehli, and P. Brennan, “The modified nodal approach to network analysis,” *IEEE Trans. Circuits Syst.*, vol. 22, no. 6, pp. 504–509, Jun. 1975, doi: 10.1109/TCS.1975.1084079.

[21] A. Gomez-Exposito, A. J. Conejo, and C. Canizares, Eds., *Electric Energy Systems: Analysis and Operation*. CRC, 2018.

[22] A. Verdicchio, P. Ladoux, H. Caron, and C. Courtois, “New Medium-Voltage DC Railway Electrification System,” *IEEE Trans. Transp. Electrif.*, vol. 4, no. 2, pp. 591–604, Jun. 2018, doi: 10.1109/TTE.2018.2826780.

[23] UNE-EN 50388:2013, “Railway Applications - Power supply and rolling stock - Technical criteria for the coordination between power supply (substation) and rolling stock to achieve interoperability,” 2002.